Characteristics of a Fast Rise Time Power Supply for a Pulsed Plasma Reactor for Chemical Vapor Destruction

Phil A. Lawless, Toshiaki Yamamoto, Sandra P. Shofran, Charles B. Boss, Carlos M. Nuñez, Geddes H. Ramsey, and Roger L. Engels

Abstract— **Rotating spark gap devices for switching high-voltage direct current (dc) into a corona plasma reactor can achieve pulse rise times in the range of tens of nanoseconds. The fast rise times lead to vigorous plasma generation without sparking at instantaneous applied voltages higher than can be obtained with dc. The resulting energetic plasma is effective for destroying a variety of molecules. The spark gap circuit configuration plays an important role in the effectiveness of the plasma generation. A single-gap circuit is effective for generating moderate peak voltages, but is limited by a multiple sparking phenomenon. A double-gap circuit can achieve equal peak voltages with every spark, but with a reduced number of pulses, compared to the single gap. Both configurations have an upper voltage imposed by the changing impedance of the reactor as voltage and frequency are varied. The pulse characteristics are reported for both types of circuits. The general performance of the reactors for destruction of some compounds with both circuits is also reported.**

Index Terms—**Corona discharge, gas cleaning, nanosecond rise time, power supply, pulsed plasma, rotating spark gap, VOC destruction.**

I. Introduction

FAST rise time dc pulses have been used to generate corona plasmas for modification or removal of trace gas species for several years [1]–[3]. From these papers, the important pulse factors that have been identified as making the plasmas effective are: 1) pulse rise times less than about 100–200 ns; 2) pulse decay times less than about 1–10 μs; and 3) peak electric fields greater than 10–20 kV/cm. The factors are interrelated, in that fast rise times result in high electric fields before the onset of corona and short decay times reduce the movement of ions, reducing the likelihood of formation of sparks in the high fields. The high electric fields that exist at the onset of corona produce higher average electron energies than can be achieved in dc coronas and are thought to lead to formation of larger numbers of energetic species and free radicals than the dc coronas can produce.

The fast rise time of the pulse is almost universally produced by switching a charged capacitor across a corona reactor by means of a spark gap. If the circuit inductance is low, rise times of less than 100 ns are easily achieved. Until recently, this was the only easily accessible technique for producing the desired pulse waveforms. (Magnetic pulse compression technologies appear capable of producing the same results, but with a considerable increase of complexity.)

Often, the spark gap has the form of rotating electrodes passing between stationary electrodes. The reasons for doing so are to control the pulse repetition rate when using a dc power supply, to distribute the erosion of the electrode faces over several different electrodes, and to sweep the ionized gases out of the spark gap to restore its insulating properties. Reliable high power switching operation is obtainable with rotating gap designs [4].

In spark gap switching, the energy storage capacitor must be isolated from the charging supply during the spark discharge to prevent a continuous power drain on the supply, long pulse tails, and possible arc formation. The isolation may be achieved with the use of resistors and inductors or by the use of separate charging and discharging spark gaps. We call the former method a "single-gap" design and the latter, a "double-gap" design. The operation of these two designs is the subject of this paper.

II. Circuit Details

Two schematic diagrams for the spark gap configurations are shown in Figs. 1 and 2. In the single-gap configuration, the dc supply is always connected across the storage capacitor, C_s, through the current limiting resistor, R_L, whose value is chosen to allow roughly 3 time constants between discharges at the highest pulse repetition rate. This ensures full charging of the storage capacitor to the applied dc voltage before each discharge. It has a value of 6–10 MΩ. In the double-gap configuration, the current limiting resistor serves to damp oscillations during the charging pulse for the storage capacitor, thereby reducing electromagnetic interference. A value of 70 kΩ (2 m of automotive spark plug wire) serves well for that purpose. At high applied dc voltages, streamers may form on

Paper MSDAD 96–8, approved by the Electrostatic Processes Committee of the IEEE Industry Applications Society for presentation at the 1993 IEEE Industry Applications Society Annual Meeting, Toronto, Ont., Canada, October 3–8. Manuscript released for publication April 15, 1996.

P. A. Lawless and T. Yamamoto are with the Research Triangle Institute, Research Triangle Park, NC 27709 USA.

S. P. Shofran and C. B. Boss are with the Department of Chemistry, North Carolina State University, Raleigh, NC 27603 USA.

C. M. Nuñez and G. H. Ramsey are with the Air and Energy Engineering Research Laboratory, USEPA, Research Triangle Park, NC 27711 USA.

R. L. Engels is with the Department of the Navy, Naval Surface Warfare Center, Dahlgren Division, Dahlgren, VA 22448-5000 USA.

Publisher Item Identifier S 0093-9994(96)06637-6.

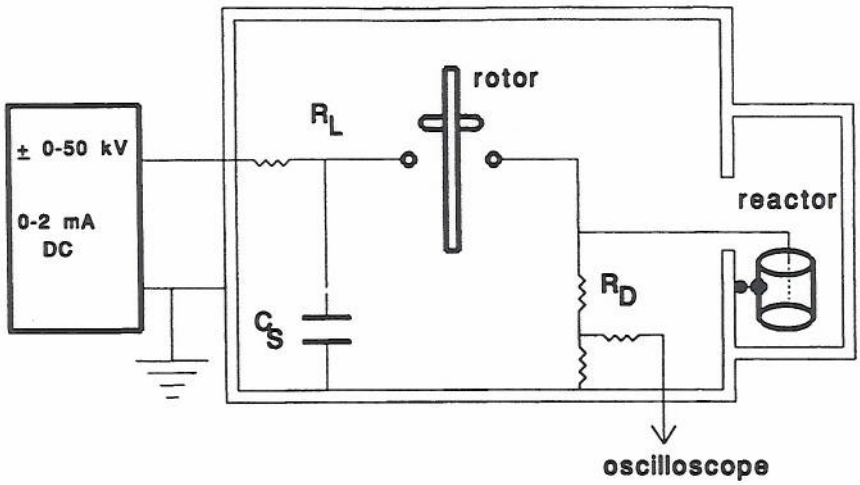

Fig. 1. Single-gap circuit schematic.

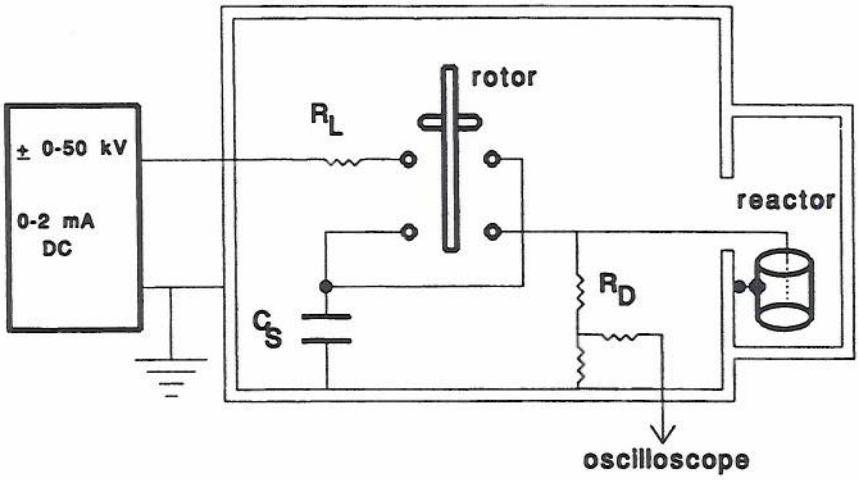

Fig. 2. Double-gap circuit schematic.

the dc portions of the circuit and spark to the walls of the supply. In such cases, increasing the value of R_L to about 1 MΩ prevents disastrous sparking, but the streamers increase the dc power consumption and the charging of the storage capacitor is not as complete.

Although the schematics clearly show that each gap is closed by a rotor electrode passing between two stationary electrodes, we call this a single gap because both sides fire simultaneously. There are eight equispaced electrodes on the rotor with only one shown for clarity.

The storage capacitor, C_s, is a critical item in the circuit. In order to minimize its intrinsic inductance, the capacitor is made as a round, flat plate (approximately 10 cm in diameter) resting on a 0.6-cm thick acrylic plastic sheet which itself rests on the wall of the shielding enclosure. The current lead is attached to the geometric center of the plate by a compression clamp. This results in a symmetrical flow of current with substantial cancellation of induced voltages, resulting in low inductance.

The capacitor discharges into a circuit composed of the coaxial plasma reactor in parallel with a resistive voltage divider, R_D in Figs. 1 and 2. The divider serves two purposes: scaling the voltage pulse for an oscilloscope and shaping the wave form of the discharge. The total value of the divider is nominally 10 kΩ; it has a 10 000 : 1 division ratio and a 50-Ω output impedance, for a total division ratio of 20 000 : 1 into a properly terminated 50-Ω line. The discharge time constant of the storage capacitor and the resistive divider is approximately 1 μs. Thus, once the spark gap fires, the full stored voltage appears across the divider and the plasma reactor and then decays to zero within about 3 μs.

The divider resistor has a third purpose, which may not be necessary. It causes the discharge current in the spark gap to rise quickly to 1–2 A at the onset of the spark. At this current level, the voltage drop in the spark itself (actually an arc, in conventional discharge terminology) becomes a negligible fraction of the applied voltage [5]. The impedance of the corona reactor has not been considered in this analysis, but may itself be sufficiently low to ensure a low gap voltage.

III. Electrical Measurement Techniques

Two types of electrical measurements have been made: dc supply voltage and current and plasma reactor pulse voltage and current. The dc measurements are not sensitive to the reactor (it can be removed from the circuit without being

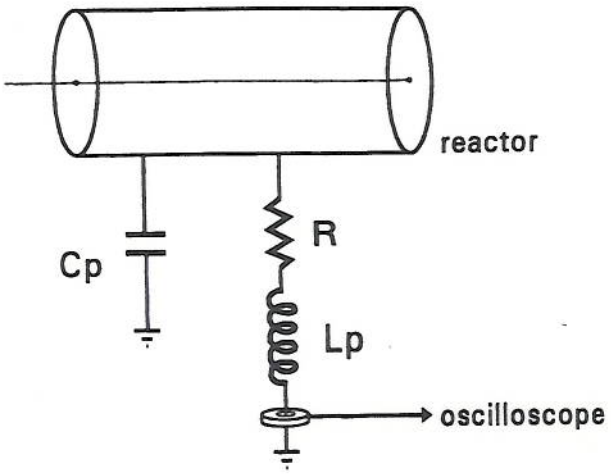

Fig. 3. Circuit for measuring current pulses.

detected in the measurements) and therefore describe the operation of the storage capacitor, spark gap(s), and the divider resistor. The dc measurements are taken from the panel meters of the power supply.

The pulse measurements directly measure the voltage applied to the reactor and the current flowing through it. They are made with a Nicolet 450 two-channel digital oscilloscope having a 5-ns-per-point time base and signal averaging capabilities.

The pulse characteristics are difficult to measure because of a wide disparity in the time scales. The total pulse width is roughly 3 μs; the electrode rotor remains close to the stationary electrodes for periods of about 500 μs, when multiple pulses may occur; and the basic repetition period is about 3 ms (300 Hz). The spark breakdown occurs with unpredictable time delays, so that the only reliable trigger for observations is the voltage pulse itself. Pulse averaging is used to smooth pulse-to-pulse variations of amplitude and phase, but the setting of the trigger level for the oscilloscope can bias the average significantly by selecting for high- or low-amplitude pulses.

The resistor voltage divider was designed for high frequency response by using a low total impedance to minimize stray capacitance effects and by placing the resistors making up the divider in a straight line to minimize their mutual inductance. The voltage pulse waveforms from the divider compared well with those from a Tektronix compensated high-voltage probe and showed a slightly faster rise time.

Although the current need not be measured, as in Figs. 1 and 2, it can provide useful information about the operation of the system. The current pulse was sampled with a current transformer, Pearson Model 2877, in Fig. 3. This replaced a resistive shunt previously used which suffered ground loop problems. The current waveform exhibited strong ringing, a result of the excitation of the parasitic parallel capacitance to ground, C_p, of the reactor body and the parasitic inductance of the current lead, L_p (Fig. 3). The oscillations were damped by placing a 1-Ω resistor, R, in series with the current lead. Combined with the signal averaging, this was sufficient to obtain reasonable waveforms.

IV. Measurements

A. Single-Gap Circuit

The dc voltage-current curve for the single-gap operation is shown in Fig. 4. Values were taken from the panel meters and were quite stable over periods of several minutes. The curve can be seen as a composite of several straightline segments, roughly indicated by the broken straight lines. This shape is characteristic of the close-spaced single gap. The onset voltage, at which current first begins to flow, is controlled by the gap spacing at closest approach. In a laboratory situation, it is advantageous to have the onset voltage as low as possible to allow phenomena to be investigated over the widest range of voltages. The initial slope of the curve is given accurately by the transfer of charge to the high voltage storage capacitor, followed by complete discharge at the nominal pulse frequency (300 Hz in this case).

As the dc voltage is raised, current flows through R_D alone until corona onset is reached at about 10 kV. The current increases with nearly constant slope until an increase of the slope occurs at about 13 kV, and again at 24 and 32 kV. Simultaneously, visual observation of the spark gaps show both long and short sparks. We propose the following explanation for these observations.

The initial slope of the V–I curve is explained by the discharge of the storage capacitor one time as the rotor electrode closes the gap. As the applied voltage is raised, the spark is initiated with the rotor farther away from the point of closest separation. When the applied voltage is high enough, the storage capacitor discharges once when the rotor is far from closest approach and has time to be recharged sufficiently for a second spark at or near the closest approach. At still higher applied voltages, the storage capacitor is capable of discharging three or more times during the passage of the rotor toward and through the point of closest approach.

Calculations of the charging rate through the current limiting resistor (R_L) show that a substantial fraction of the applied voltage can be delivered to the storage capacitor in the time between the first spark and the point of closest approach. Since the gap distance is much shorter at closest approach and since it has been preconditioned by the initial spark, there is a strong likelihood of a second breakdown during each passage of the rotor through the gap. However, the secondary sparks occur at a lower voltage, so that the pulses delivered to the reactor are both the high voltage of the initial spark and the lower voltage of the secondary spark or sparks.

These secondary voltage pulses have been observed with an analog oscilloscope (Tektronix 547); the secondary pulses are visible between the primary pulses, even though they cannot be completely resolved. As expected, the secondary pulses are lower in amplitude than the primary pulse.

Depending on the method of triggering the oscilloscope, this mixture of voltage pulses can show up as an average pulse voltage that does not increase as fast as the applied dc voltage. For example, if the trigger level is set at the lower part of the voltage waveform, all pulses would be averaged together, giving an average amplitude between that of the initial spark and the secondary spark. If the trigger level is set at the upper

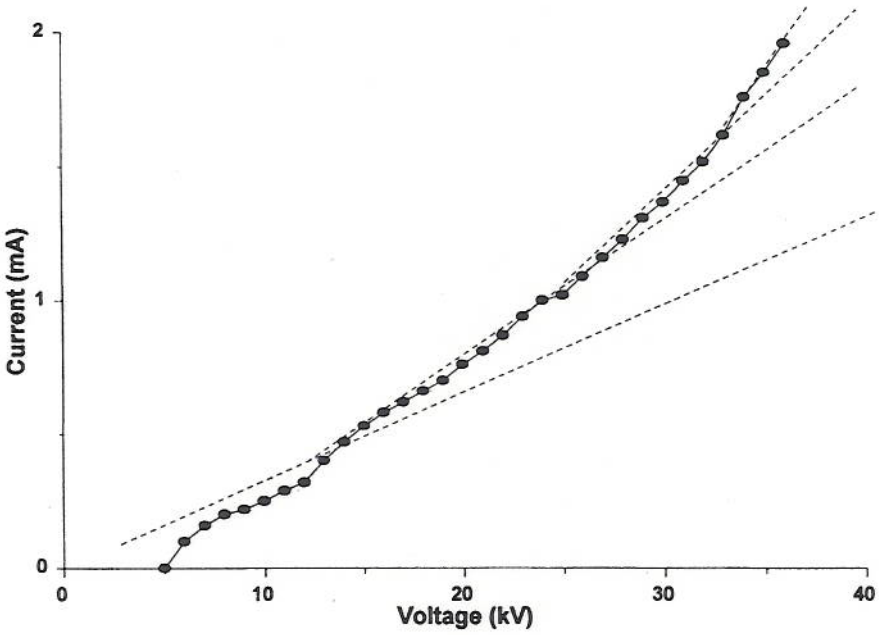

Fig. 4. V–I curve for single-gap operation.

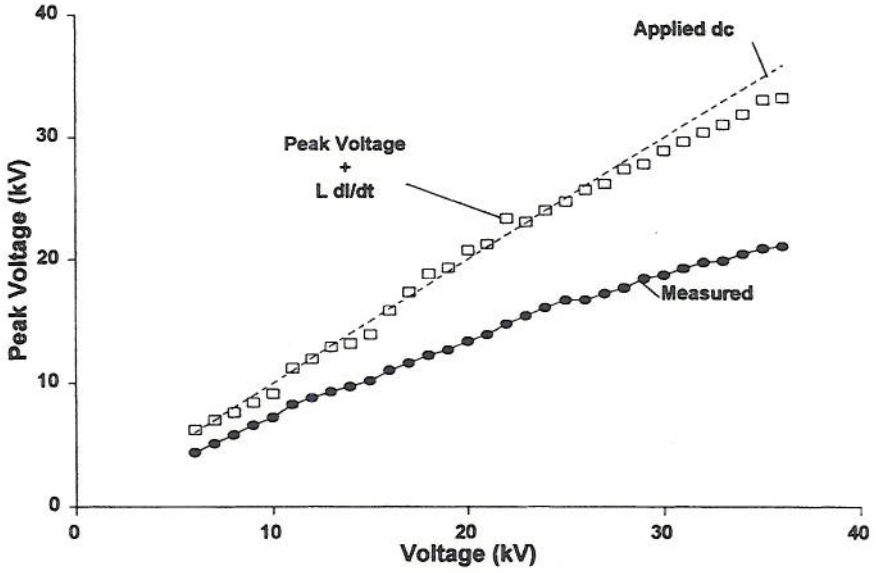

Fig. 5. Voltage pulse peak amplitude.

part of the pulse waveform, then many of the secondary pulses will not be included in the average. If the trigger level is set by the peak of the current waveform, then weak current pulses, coming from low-voltage sparks, would be excluded from the average.

Fig. 5 shows the peak amplitude of the voltage pulses compared to the applied dc voltage, as measured using a current pulse trigger. The broken line shows the amplitude expected if the full dc voltage could be delivered with each spark. The average slope of the measured peak voltages is lower than the theoretical curve's and in addition, the slope of the measured curve slowly decreases throughout its length. Although this would be expected if increasing numbers of low voltage sparks were averaged with the high voltage sparks, triggering on the peak current should not include the lower amplitude voltage pulses. Instead, an explanation that fits the observation is that the peak voltage is limited by a voltage drop across the stray inductances of the circuit. The open squares in Fig. 5 portray the voltage applied across the divider resistor and a series inductance of 11 μH, as calculated from the measured peak current and a measured risetime of 20 ns. The match to the applied dc voltage is quite good.

The averaged peak current is expected to consist of current pulses mainly from the high-voltage discharges, as determined by the trigger threshold. As seen in Fig. 6, the peak current increases to about 20 A, with a plateau region below 10 kV. Below 10 kV, visual observation shows no corona formed in the reactor. Therefore, over that range, the current

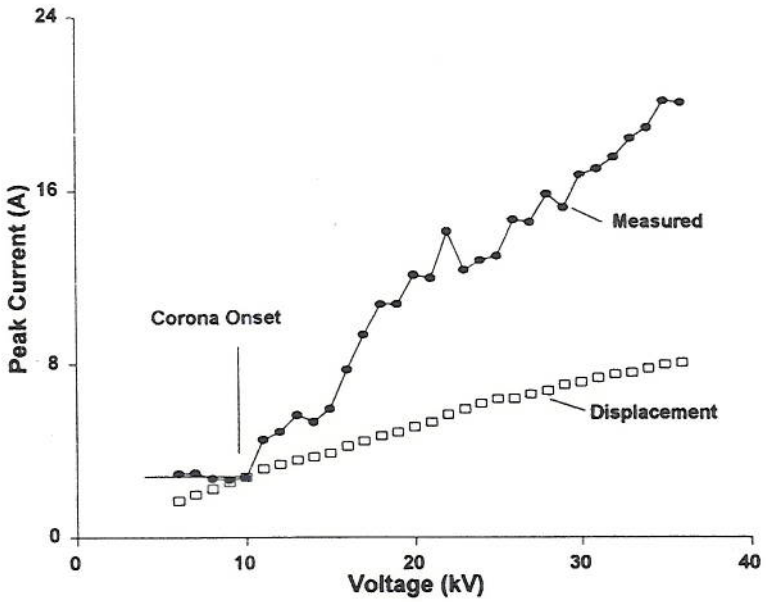

Fig. 6. Current pulse peak amplitude.

pulses represent the coupling of the voltage pulse through the capacitance of the reactor. Calculations of the displacement current through reactor capacitance due to the rate of change of applied voltage give good agreement with the measured current peaks at 10 kV, as shown by the broken line. Below 10 kV, the displacement current should decrease as indicated; the apparent plateau is probably due to the difficulty of obtaining a good measurement with the strongly ringing wave form. Above 10 kV, the measured current increases faster than the displacement current, indicating the onset of plasma generation. The presence of the plasma space charge changes the effective voltage driving the displacement current so that it is not possible to separate the real and displacement currents above 10 kV by subtraction, even though a calculated value is shown.

By comparing the averaged peak currents in Fig. 6 with the curve in Fig. 4, we see that the slope changes on the V–I curve at 13 and 24 kV correspond to drops in peak current amplitude. These crossover points are voltages at which the number of sparks per pass increases by one, producing a mixture of low- and high-amplitude current pulses. Although the trigger setting eliminates most of the low-amplitude pulse, enough are averaged in the reading to produce the slight amplitude decreases shown.

B. Double-Gap Circuit

In the double-gap circuit, the storage capacitor is charged at one gap and discharged at the second. This isolates the reactor load from the dc supply. It also prevents the occurrence of multiple sparks because there can be no charging of the storage capacitor while the rotor electrode is near the reactor discharge gap.

The V–I curve for the double gap is expected to be very linear with voltage, and as seen in Fig. 7, it is, over much of the range. The onset of sparks that charge the storage capacitor occurs at about 9–10 kV, higher than before because of residual charge on the storage capacitor after it discharges. At higher dc voltages, the sparks in both gaps are more intense so that the storage capacitor probably approaches full discharge with each pass. The slope of the V–I curve with the double gap is approximately two-thirds the slope of the low-voltage portion of the single-gap curve. The reason for this is not known, but two possibilities exist. One is that dc supply must charge the storage capacitor through stray circuit inductance in a short time, leading to a voltage drop of the same order as detected in the discharge of the single-gap circuit. The other possibility is that the voltage drop across the gap during the charging spark is proportional to the length of the spark and is of the order of several thousand volts; this is contraindicated in [5].

The amplitude of the peak voltage is shown in Fig. 8. The amplitude shows a much slower increase with dc voltage than the single-gap amplitudes do. The broken line in Fig. 8 represents the applied dc voltage. The open squares represent the sum of the peak voltage across the reactor and two correction terms: an $L\,dI/dt$ term, as before, and the average voltage drop across the current limiting resistor. The inductive voltage drop uses an effective inductance of 16.5 μH, a value estimated from the fact that the charging *and* discharging currents must both flow through part of the capacitor leads, and the discharge current must flow through an additional length of wire. The average voltage drop across the limiting resistor accounts for the limitation of current available for charging. These corrections account quite well for the losses in transferring the dc voltage to the peak voltage across the capacitor.

Since the double-gap circuit was designed to reduce the production of multiple sparks, which it does fairly well, we find the slow rate of increase of the peak voltage disappointing. The double-gap circuit reduces the averaging of high- and low-voltage sparks and provides a well-defined pulse rate, but at the expense of pulse amplitude.

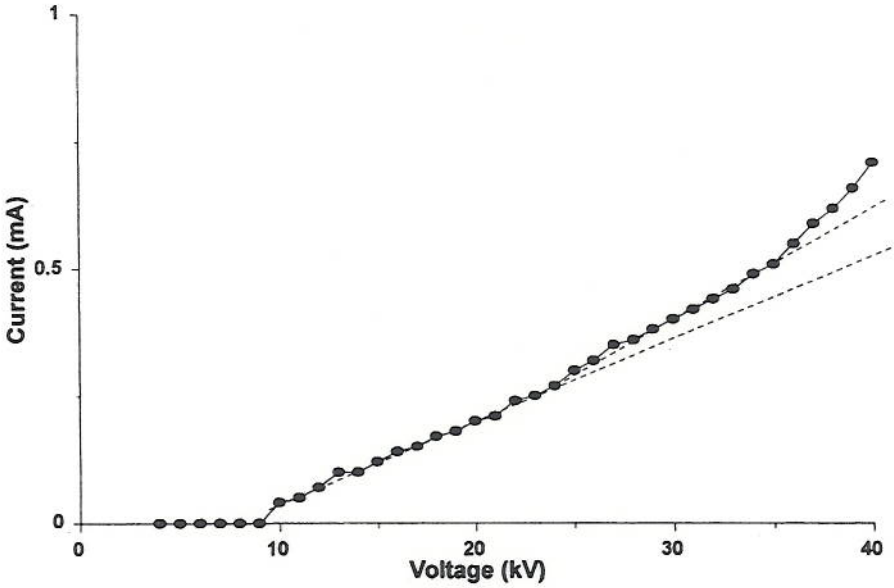

Fig. 7. V–I curve for double-gap circuit.

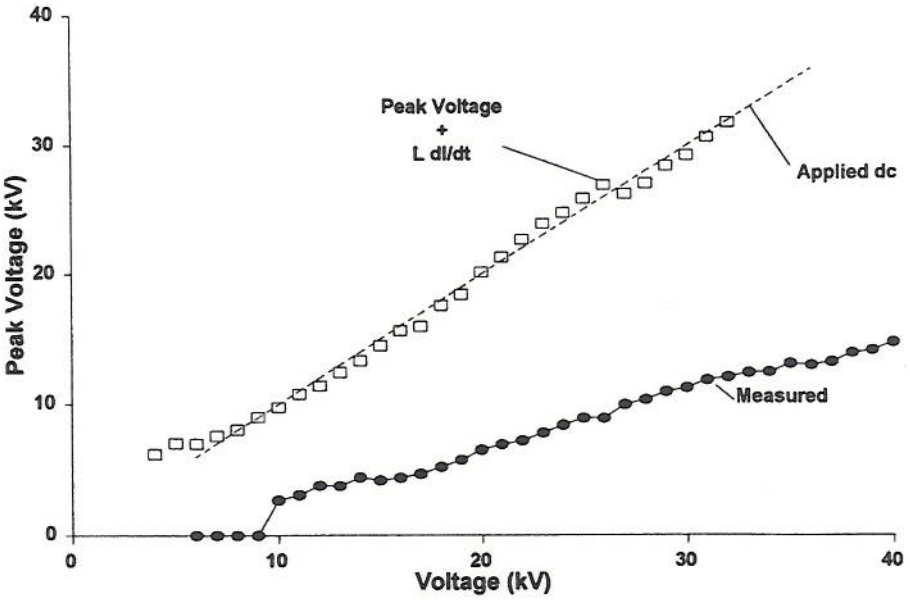

Fig. 8. Peak voltage amplitdue for the double-gap circuit.

The amplitude of the peak current as a function of dc voltage is shown in Fig. 9. The corona onset is at an applied voltage of 20 kV, and the calculated displacement current agrees well with the measured current below that voltage. The double-gap circuit current pulses are somewhat lower than those measured in the single gap, for the same voltage difference above the corona onset value. This is consistent with the lower peak voltage in the double-gap circuit compared with the single-gap circuit for the same difference in dc voltage. The current pulse amplitude shows a pronounced drop 36 kV in Fig. 9. There is a change in slope of the V–I curve at that voltage in Fig. 7, indicating the addition of a secondary spark at that point.

V. Transition Effects

These curves were measured with a low concentration (200 ppm) of Freon 113 in the gas stream. The presence of the Freon suppresses an impedance transition that we observe consistently in air and other gases that complicates the electrical operation of the pulse corona reactor. In air at applied voltages of 26–28 kV, the peak voltage amplitude actually drops, both as a function of voltage and of time. This is a property of the gas, because the voltage at which it appears can be raised by pressurizing the gas in the reactor and is a function of gas composition.

Up to the onset of this transition, the voltage pulse shows the typical exponential decay characteristic of the resistive divider and the storage capacitor. When this transition point is reached, the voltage pulse decays much more rapidly and is nearly zero within about 100 ns. The current amplitude is not affected noticeably and continues to increase with applied voltage.

Among other effects associated with the transition, the rate of ozone generation decreases by up to three orders of

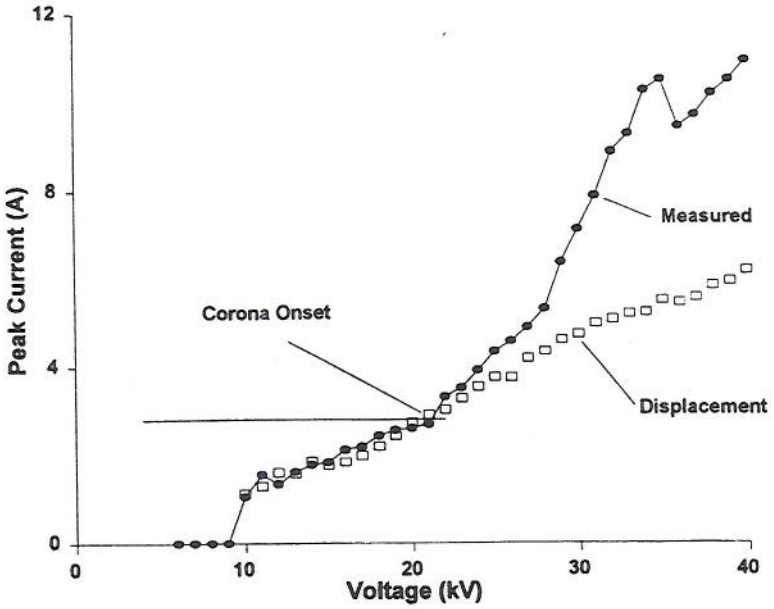

Fig. 9. Peak current amplitude for the double-gap circuit.

magnitude and the rate of NO_x generation increases by an order of magnitude.

VI. Reactor Effectiveness

The plasma reactor is being used to study the removal of low concentrations of volatile organic compounds of various types from gas streams. One of the more thoroughly studied compounds has been toluene, which is relatively easy to destroy. Although it is desirable that hydrocarbons such as toluene be completely reduced to water and carbon dioxide, for the following discussion, we use "destruction" to mean the reduction of concentration of the compound of interest.

The toluene is delivered at a fixed concentration in a tank of compressed, simulated air. It is flowed through the reactor with no voltage applied to calibrate the gas chromatograph with flame ionization detector used in the measurements. Then, the dc supply voltage is raised in steps and the concentration emerging from the reactor is determined.

At voltages below the corona plasma onset, roughly 10-kV dc for the reactor used with single gap, the displacement current pulses are detected but no destruction of the toluene or ozone generation takes place. Commencing at the plasma onset, increasing amounts of toluene are destroyed and ozone is produced as the dc voltage is raised. If the initial concentration is low enough or sufficient treatment time is allowed, complete removal can be obtained. If the voltage is raised still further, until the transition to the lower plasma impedance occurs, the removal is reduced and a measurable fraction of the toluene emerges from the reactor. Further increases in dc voltage slowly increase the fraction removed, but complete removal is usually not possible.

The removal of toluene appears to be governed by the formation of a reactive radical in the gas, rather than by a direct interaction with the plasma. If the interaction were direct, then the fraction removed would be independent of concentration for a fixed set of electrical conditions. Instead, it is observed that fixed electrical conditions remove roughly the same quantity of toluene, independent of concentration.

Unfortunately for the comparison of the spark gap circuits, we do not have measurements in the same reactor. The single-gap measurements were performed in a first-generation reactor and the double-gap measurements were performed in a second-generation reactor about twice as long as the first. For equal flow rates, the treatment time in the first reactor was about half that in the second. However, treatment time is not critical if sufficient quantities of the reactive radical are produced, but if the generation rate is low, the extra time spent in the reactor allows more molecules to react.

The single-gap circuit and reactor were able to remove 48 ppm of toluene (out of 48 ppm challenge) with a dc voltage 9 kV above the corona onset at a flow rate of 0.75 l/m through the reactor. The double-gap circuit and reactor, using a 108 ppm challenge at a flow rate of 1.5 l/m for comparable treatment times, was able to remove 39 ppm at about 12 kV above the plasma onset voltage. On the basis of this comparison, the single-gap circuit is seen to be more effective in two ways: the dc voltage at plasma onset is significantly lower and the peak voltage increases more rapidly with the dc voltage than in the double-gap circuit. As a result, the single-gap reactor removes slightly more toluene than the double-gap reactor at a significantly lower dc voltage, even though the peak voltages are roughly comparable and the average dc currents are about the same.

Another measure of the reactor effectiveness is the conversion of the hydrocarbons into CO_2. If the conversion were complete, the concentration of CO_2 would be seven times the concentration of toluene removed, because of the seven carbon atoms in the toluene molecule. In actuality, significant fractions of CO are produced as well, so that the

carbon balance should include the sum of the CO and CO_2 components.

Generally, both circuits and reactors can convert the toluene completely into the carbon oxides, provided the applied voltage can be raised sufficiently beyond the point at which complete removal of the toluene takes place. (The impedance transition that reduces the toluene removal also reduces the amount of CO and CO_2 produced.) Neither reactor has proved able to convert the CO completely into CO_2 over the voltage range allowed at challenge concentrations of 50 ppm or greater.

The single-gap circuit, however, generally produces CO_2 at 2 to 3 times the concentration of CO, over a wide range of voltages. In contrast, the double-gap circuit produces more CO than CO_2 over the full operating range. Near the plasma onset, the CO concentration may be as much as seven times the CO_2 concentration. In the range where the toluene is not completely removed, the CO concentration is roughly two times the CO_2 concentration. Only when the toluene is fully removed do the CO and CO_2 concentrations become roughly equal.

Clearly, the oxidation of CO to CO_2 requires an energetic radical that is in limited availability in the double-gap reactor. It is reasonable to suppose that the CO is in competition with the toluene for the consumption of the radical. The performance of the single-gap reactor with regard to the better conversion of CO to CO_2 is a strong indication that the production rate of the radical is much higher than in the double-gap reactor.

It is likely that a combination of factors enhances the production rate in the single-gap reactor. The first is the higher peak voltages available, because the average electron energy in the plasma increases with higher applied fields at the initiation of the plasma formation process. The second factor is the formation of the multiple sparks in stages as the dc voltage is raised. Even though the peak currents decrease slightly with multiple sparks, the increased frequency of the sparks raises the power delivered to the gas and should result in a direct increase of the amount of radical produced.

VII. Conclusion

When we compare the two circuits and reactors on the basis of pulse voltage, pulse current, and actual frequency of pulses, there seems to be little difference in the reactor effectiveness for the removal of toluene. When we compare the reactor effectiveness in terms of the dc supply, the single-gap circuit achieves its effective operation at a considerably lower dc voltage than the double-gap circuit does. If we limit the operating point to the voltage at which complete removal of the toluene occurs, the average dc currents of the two circuits are comparable. If we raise the voltage beyond the point of complete removal to enhance the conversion of CO to CO_2, the current consumption in the single-gap supply rises much faster than it does in the double-gap supply, but the conversion rate also rises faster.

As a result, in the laboratory, the single-gap supply provides a wider range of operating parameters than the double-gap supply does, but it is more difficult to characterize the pulses with regard to frequency and amplitude than with the double-gap supply.

The slow rate of increase of pulse voltage amplitude with applied dc voltage in the double-gap supply, identified as a function of the circuit inductance, can become a serious limitation on the effectiveness of the double-gap supply. It seems clear that this inductance limitation would apply in larger scale units, because the pulse currents must pass through some of the inductance twice, once on charging and once on discharging.

References

[1] A. Mizuno, J. S. Clements, and R. N. Davis, "A method for the removal of sulphur dioxide from exhaust gas utilizing pulsed streamer corona for electron energization," *IEEE Trans. Ind. Applicat.*, vol. IA-22, pp. 516–522, 1986.

[2] S. Masuda and H. Nakao, "Control of NO_x by positive and negative pulsed corona discharge," in *Conf. Rec. IEEE-IAS Annu. Meet.*, Denver, CO, Sept. 28–Oct. 3, 1986, pp. 1173–1189.

[3] S. Masuda, Y. Wu, T. Urabe, and Y. Ono, "Pulse corona induced plasma chemical process for $DeNO_x$, $DeSO_x$ and Mercury vapor control of combustion gas," in *Third Int. Conf. Electrostatic Precipitation*, M. Rea, Ed., Abano, Italy, 1987, pp. 667–676.

[4] J. Rasmussen, "High power short duration pulse generator for SO_x and NO_x removal," in *Conf. Rec. IEEE-IAS Annu. Meet.*, San Diego, CA, Oct. 1–5, 1989, pp. 2180–2184.

[5] J. D. Cobine, *Gaseous Conductors*. New York: Dover, 1958, p. 293.

Phil A. Lawless received the B.A. degree in physics from Rice University, Houston, TX, in 1965, and the Ph.D. degree in physics from Duke University, Durham, NC, in 1974.

Since then, he has been with the Research Triangle Institute, Research Triangle Park, NC, in many fields. He has worked in aerosol science areas for many years. A leading electrostatic precipitator modeler, he has published computer programs and papers on electrostatic precipitator phenomena. The pulse plasma technology is a natural extension of that work and shares many of the same multidisciplinary challenges. He has recently been engaged in personal exposure monitoring and application of control of particles and VOC's in indoor air.

Toshiaki Yamamoto received the Ph.D. degree in mechanical engineering from The Ohio State University, Columbus.

He is a Senior Research Mechanical Engineer, Research Triangle Institute, Research Triangle Park, NC, leading various projects relating to nonthermal plasma technology, microcontamination control, computational fluid dynamics, and indoor air pollution control research. Prior to joining RTI, he was an Adjunct Professor in the Department of Engineering, as well as Research Engineer, Denver Research Institute, University of Denver, Denver, CO. He is the author of more than 200 published works.

Dr. Yamamoto is a member of Sigma Xi, IEJ, and JAAST.

Sandra P. Shofran was born in North Wilkesboro, NC, in 1968. She received B.S. and M.A. degrees in 1990 and 1991 in chemistry from the College of William and Mary, Williamsburg, VA. She did graduate and undergraduate research under Dr. G. W. Rice and is currently doing graduate research at North Carolina State University, Raleigh, under the direction of Dr. C. B. Boss. Her research is a study of the corona discharge, focusing on plasma characteristics and reaction mechanisms.

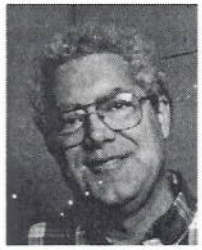

Charles B. Boss received the B.S. degree in chemistry in 1968 from Wake Forest University, Winston-Salem, NC, and the Ph.D. degree in analytical chemistry in 1977 from Indiana University, Bloomington.

In 1977, he joined the chemistry faculty of North Carolina State University, Raleigh. His principal research interests are in plasma and flame ionization of chemical samples.

Carlos M. Nuñez received the B.S. degree in both chemical engineering and chemistry from the University of Puerto Rico, Rio Piedras, and the M.S. degree in material science and engineering from North Carolina State University, Raleigh.

He is a Senior Research Engineer with 11 years of experience in research and development in air pollution control and prevention at the U.S. Environmental Protection Agency. His present responsibilities include leading and organizing research in low-emission coatings and reinforced plastics. He is the team leader of the Pollution Prevention Team for the National Risk Management Research Laboratory's Air Pollution Prevention and Control Division, Research Triangle Park, NC.

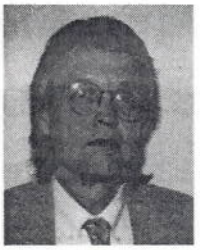

Geddes H. Ramsey received the B.S. degree in chemical engineering from the Virginia Polytechnic Institute and State University, Blacksburg.

He has 21 years of experience in research and development in air pollution control and the U.S. Environmental Protection Agency. His experience has included developing and evaluating control devices for particulates and air toxics. He is currently involved with pollution prevention of volatile organic compounds in the areas of reinforced plastics, auto body refinishing, and depainting in the aerospace industry.

Roger L. Engels received the B.S. degree in physics from Illinois College, Jacksonville, in 1962.

He is a physicist in the Chem-Bio Systems Analysis Branch of the Naval Surface Warfare Center, Dahlgren Division, Dahlgren, VA, where he has worked since 1963. In addition to electrical discharge destruction of chemicals, he has directed work on chemical detection and aerosol measurement projects related to chemical defense. He has recently directed measurements of aerosol penetration of clothing and serves on a Department of Defense working group establishing test methods for chemical protective clothing.

IEEE TRANSACTIONS ON

INDUSTRY APPLICATIONS

A PUBLICATION OF THE IEEE INDUSTRY APPLICATIONS SOCIETY

SERVING OUR MEMBERS AND SUBSCRIBERS IN OUR THIRTY-SECOND YEAR OF PUBLICATION

NOVEMBER/DECEMBER 1996 VOLUME 32 NUMBER 6 ITIACR (ISSN 0093–9994)

(Continued on page 1225)